

# Homeostatic competition drives tumor growth and metastasis nucleation

Markus Basan, Thomas Risler,\* and Jean-François Joanny  
*Laboratoire Physico-Chimie Curie (CNRS-UMR 168, Université Pierre et Marie Curie Paris VI),  
Institut Curie Centre de Recherche, 26 rue d'Ulm, F-75248 Paris Cedex 05, France*

Xavier Sastre-Garau  
*Département de Biologie des Tumeurs, Institut Curie,  
26 rue d'Ulm, F-75248 Paris Cedex 05, France.*

Jacques Prost  
*Laboratoire Physico-Chimie Curie (CNRS-UMR 168,  
Université Pierre et Marie Curie Paris VI), Institut Curie Centre de Recherche,  
26 rue d'Ulm, F-75248 Paris Cedex 05, France and  
E.S.P.C.I., 10 rue Vauquelin, F-75231 Paris Cedex 05, France*

We propose a mechanism for tumor growth emphasizing the role of homeostatic regulation and tissue stability. We show that competition between surface and bulk effects leads to the existence of a critical size that must be overcome by metastases to reach macroscopic sizes. This property can qualitatively explain the observed size distributions of metastases, while size-independent growth rates cannot account for clinical and experimental data. In addition, it potentially explains the observed preferential growth of metastases on tissue surfaces and membranes such as the pleural and peritoneal layers, suggests a mechanism underlying the seed and soil hypothesis introduced by Stephen Paget in 1889 and yields realistic values for metastatic inefficiency. We propose a number of key experiments to test these concepts. The homeostatic pressure as introduced in this work could constitute a quantitative, experimentally accessible measure for the metastatic potential of early malignant growths.

## Introduction

The progression of cancer is a multi-step process. Over 80% of malignant tumors are carcinomas that originate in epithelial tissues from where they invade through the basal membrane into the connective tissue. At some point, subpopulations of cells may detach from the primary tumor and spread via the bloodstream and the lymphatic system. Some of them give rise to metastases in distant organs. Metastases account for the majority of patients' deaths due to cancer, and thus understanding the metastatic process is of critical importance. The metastatic cascade is a very inefficient process, as only one in about a thousand cells that leave the primary tumor goes on to form a macroscopic secondary tumor. This property is referred to as “metastatic inefficiency” (Chambers *et al.*, 2002; Sahai, 2007). Recent experimental results have shown however that cell extravasation is highly efficient, namely that over 80% of the metastatic cells that are present in the bloodstream manage to enter a distant organ (Luzzi *et al.*, 1998; Cameron *et al.*, 2000; Zijlstra *et al.*, 2002). Thus, the main contribution to metastatic inefficiency arises from the failure of cancerous cells to grow inside invaded organs. Metastatic tumors also show preferential growth in different organs with a distribution that cannot be explained by blood flow patterns alone. Hence, the ef-

iciency of the metastatic process depends on specific interactions between the invading cancer cells and the local organ tissues (Fidler *et al.*, 2003). This concept, referred to as the “seed and soil hypothesis”, was introduced by Stephen Paget as early as 1889 (Weinberg, 2007): “the seed”—the metastatic cell—needs to be compatible with “the soil”—the host tissue—for successful growth to occur (Fidler, 2003; Couzin, 2003). Despite this early observation, the nature of the interactions controlling both the efficiency of the metastatic process and its tissue specificity remains a poorly understood aspect of cancer progression even today.

In this work, we introduce the notion of homeostatic pressure and propose that it is an important property for describing the competition between different tissues grown in a finite volume. The concept of homeostatic pressure is best defined from the following experiment: consider a chamber in which cells can be cultured with a setup that enables successful proliferation, allowing in particular for water, oxygen, nutrients and growth factors to diffuse through the compartment walls, keeping the cells' biochemical environment constant. The compartment is closed on one side by a piston connected to a rigid wall with a spring (Fig. 1A). As the growing tissue fills the available space and gradually compresses the spring, the pressure rises until a steady state is reached in which division balances apoptosis and the piston stops moving. The spring position is stable, since further growth increases the pressure above this value and favors apoptosis, whereas recession of the piston decreases the pressure and favors division. This steady state is characterized by

---

\*Electronic address: thomas.risler@curie.fr

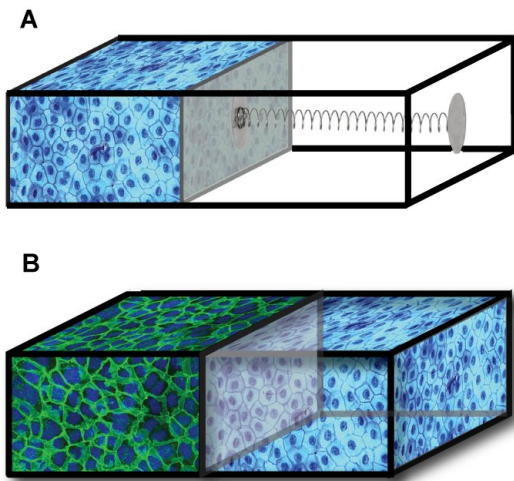


FIG. 1: (A) Schematic representation of a measurement apparatus for the homeostatic pressure. As the tissue proliferates, the piston compresses the spring and the pressure exerted on the tissue increases. Once a steady state is reached, cell division and apoptosis balance. The cell density and the pressure exerted on the spring at this point define the homeostatic mechanical state of the tissue in a given biochemical environment. (B) Schematic representation of a tissue-competition experiment. The two tissues are in mechanical contact through a freely-moving, impermeable piston. The tissue with the lower homeostatic pressure is compressed to a cell density above its homeostatic point and initiates apoptosis. The other tissue proliferates and expands until the opposing tissue has disappeared.

a well-defined pressure exerted on the spring and a well-defined density of cells, which we refer to as the homeostatic pressure and density of the tissue in this particular biochemical environment. Note that the homeostatic pressure is different from the hydrostatic pressure since the lateral walls of the chamber allow for fluid transport. Instead, it resembles more an osmotic pressure but originates from the forces driving tissue expansion.

We now show that the ability of one tissue to replace another one in a competition for space depends on the relative values of their homeostatic pressures. Let us consider a similar chamber, but in which the piston separates two tissue compartments  $H$  and  $T$ , establishing mechanical contact (see Fig. 1B). Suppose that tissue  $H$  has a homeostatic pressure  $p_{H,h}$  smaller than that of tissue  $T$ ,  $p_{T,h}$ . As cells divide, the pressure rises and first reaches the homeostatic pressure  $p_{H,h}$ . At this point, tissue  $H$  stops growing while tissue  $T$  continues to proliferate and drives the pressure above  $p_{H,h}$ . As a result, the apoptosis rate of  $H$  becomes larger than its division rate, resulting in its recession. The process continues until tissue  $H$  completely disappears. The winning compartment always corresponds to the tissue with the larger homeostatic pressure.

It is interesting to consider the effect of biochemical signaling or immunological interactions between the two

tissues. In particular, consider the case where  $H$  resists the expansion of  $T$  by locally decreasing the homeostatic pressure of  $T$ . If this decrease is large enough, tissue  $T$  shrinks and the result of the competition will be reversed as compared to the case without signaling. However, if we consider a sufficiently large compartment  $T$ , the region close to  $H$  has a negligible contribution to the overall compartment growth, and  $T$  expands as in the absence of signaling. There is a particular size of compartment  $T$  for which, at the homeostatic pressure  $p_{H,h}$ , its average growth vanishes: the excess division away from the piston exactly balances the excess death close to it. A steady state is possible for this particular size of compartment  $T$ , but it is unstable. This introduces the second important concept of this paper: the existence of a critical size beyond which a tumor tends to grow and below which it tends to shrink.

A critical size can also exist due to interfacial tension in higher-dimensional geometries, such as the two-dimensional organisation of a monolayered epithelium or the three-dimensional configuration of a secondary tumor within the bulk of a host tissue. The concept of tissue interfacial tension has already been used to explain cell sorting of tissues with different adhesive properties (Duguay *et al.*, 2003), and quantified for several tissues (Foty, 1996). Tissue interfacial tension can also originate from the mechanical contraction of cytoskeletal elements at the interface (Lecuit and Lenne, 2007; Schötz *et al.*, 2008). In a spheroid of tissue  $T$  located within the bulk of tissue  $H$ , the excess pressure in  $T$  is given by Laplace's law:  $\Delta p = 2\gamma/r$ , where  $\gamma$  is the interfacial tension between  $H$  and  $T$  and  $r$  is the radius of the spheroid. As a result, for small enough radii, the pressure in  $T$  is larger than  $p_{T,h}$ , and  $T$  recedes. For large radii however, the excess pressure as given by Laplace's law vanishes and we recover the previous one-dimensional case where  $T$  grows. There is again an unstable critical radius  $r_c$  for which a steady state exists.

So far, we have considered cell growth and death processes as entirely deterministic, in which case only tumors larger than the critical size can grow. However, single cells give rise to tumors and metastases (Talmadge and Fidler, 1982; Talmadge and Zbar, 1987; Chambers and Wilson, 1988). This is possible because cell growth and death are stochastic processes. In this paper, we calculate the probability for a single cell to give rise to a macroscopic tumor and obtain results that are compatible with experimental data on metastatic inefficiency (Luzzi *et al.*, 1998; Cameron *et al.*, 2000; Zijlstra *et al.*, 2002). The concepts we use here are similar to those used to describe the statistics of nucleation processes as they occur in first-order phase transitions. It is well known that nucleation is easier on surfaces or foreign bodies than in the bulk of a system. The same holds true for tumor growth: we show that it is more likely for tumors to reach the critical size at an interface than in the bulk of a tissue, in agreement with experimental and clinical observations (Cameron *et al.*, 2000; Weiss, 1985). Hence, in this pa-

per, we argue that an unstable critical size for tumor growth exists, which is responsible for the inefficiency of the metastatic cascade and could account for the preferred growth of metastases on surfaces and interfaces. We treat only the early stages of tumor and metastatic growth, where the heterogeneity of tumors—due to effects such as the diffusion of nutrients and growth factors or genetic mutations—can be neglected. These effects play an important role for larger tumor sizes only (Hanahan and Weinberg, 2000).

## Results

### Tissue Rheology and Homeostasis

While the notion of homeostatic pressure and density is model independent, the details of the tissue dynamics are not. Here, we employ a continuous description that we expect to be valid for systems large compared to the cell size and time scales large compared to the characteristic times of individual cellular processes. The local density of cells  $\rho$  obeys the continuity equation:

$$\frac{\partial}{\partial t}\rho + \nabla \cdot (\rho \mathbf{v}) = (k_d - k_a)\rho, \quad (1)$$

where  $\mathbf{v}$  denotes the local velocity of the tissue and  $\nabla \cdot (\rho \mathbf{v})$  the divergence of the cell flux. The right hand side corresponds to source and sink terms that describe the local production and destruction of cells due to cell division ( $k_d$ ) and apoptosis ( $k_a$ ). In addition, tissues must also satisfy momentum conservation, which, for systems where inertia plays a negligible role, reduces to force-balance:

$$\partial_\alpha \sigma_{\alpha\beta} = 0. \quad (2)$$

Here,  $\partial_\alpha$  denotes the partial derivative with respect to the coordinate  $\alpha$  ( $\alpha = x, y, z$ ), and summation over repeated indices is implicit;  $\sigma_{\alpha\beta}$  denotes the total stress tensor that we split into a velocity-independent part and a dynamic part  $\sigma'_{\alpha\beta}$ . For an isotropic tissue, the velocity-independent part reads  $-p\delta_{\alpha\beta}$ , where  $p$  is the tissue pressure discussed above. The viscous part however encodes the rheological properties of the tissue in a constitutive equation that relates it to the velocity-gradient tensor  $\partial_\alpha v_\beta$ . Tissues are complex media with a rheological behavior intermediate between those of liquids and solids (Foty *et al.*, 1994; Schötz *et al.*, 2008). On timescales short compared to their viscoelastic relaxation time, tissues have a finite shear modulus  $E$  of the order of  $10^2$ – $10^4$  Pa (Forgacs *et al.*, 1998; Engler *et al.*, 2004; Kong *et al.*, 2005). For time scales exceeding the largest relaxation time  $\tau$  however, viscoelastic media behave as viscous liquids with viscosity  $\eta = E\tau$ . Measurements of the mechanical response of various cell aggregates suggest a value of the relaxation time in the range of tens of seconds to several minutes (Forgacs *et al.*, 1998; Schötz

*et al.*, 2008), corresponding to a viscosity in the range of  $10^3$ – $10^5$  Pa·s. The fastest division rates of mammalian cells are typically of the order of one division per day (Weinberg, 2007). Hence, tissue-growth dynamics takes place on time scales that are long compared to the characteristic times of cellular processes, including adhesion and detachment of the proteins that insure the integrity of the tissue under consideration. Under such conditions, it is a general result that the effective rheology on large scales appears to be that of a fluid (Frisch *et al.*, 1985). We therefore argue that, in the context of tissue-growth dynamics, a purely viscous rheology is appropriate, which leads to the standard constitutive equation:

$$\sigma'_{\alpha\beta} = \eta (\partial_\alpha v_\beta + \partial_\beta v_\alpha). \quad (3)$$

Under fixed biochemical and biophysical conditions, division and apoptosis rates—as well as pressure—are functions of cell density only. In the absence of a detailed knowledge of the pressure and rate dependences as functions of  $\rho$ , and for the sake of simplicity, we rely on an expansion to first order in  $\rho - \rho_h$  around the homeostatic density  $\rho_h$ :

$$\begin{aligned} p &= \chi^{-1}(\rho - \rho_h) + p_h \\ k_d - k_a &= -\kappa(\rho - \rho_h). \end{aligned} \quad (4)$$

The parameter  $\chi$  is equivalent to the standard compressibility of a material and describes the variation of cell density with pressure. Similarly, the coefficient  $\kappa$  quantifies how the difference between division and apoptosis rates depend on density. Both  $\chi$  and  $\kappa$  are experimentally accessible parameters that must both be positive to insure stability. In Eqs. (4), the expansion of the pressure  $p$  in terms of the cell density  $\rho$  is complementary to the expansion of  $k_d - k_a$  known as logistic growth, which is a common way to model growth dynamics (Sachs *et al.*, 2001). As we have stated, the most general dependence of the pressure  $p$  as well as of the division and apoptosis function  $k_d - k_a$  on the biochemical environment of the tissue is encoded in the expansion coefficients  $\chi$  and  $\kappa$  here, which are therefore constants only under fixed biochemical conditions. As we focus here on tumors of small sizes under steady environmental conditions, such a dependence will not be discussed here. But our framework in principle allows to study more complex situations where spatio-temporal inhomogeneities would play a role, simply by allowing  $\chi$  and  $\kappa$  to vary. Cell division and apoptosis could also be coupled directly to pressure, leading to tissue competition as proposed in a similar model by B. Shraiman (Shraiman, 2005). Also, studies have shown that a defective density sensing of cancerous cells can lead to a growth advantage (Chaplain *et al.*, 2006). In this paper, we argue that competition for volume is a generic property of tissues in mechanical contact, since the pressure and effective growth rate functions take the form of Eqs. (4) close to the steady state density of the tissue.

## Tumor Growth Dynamics

We are now in a position to show that homeostatic regulation intrinsically contains a growth mechanism for neoplastic tissues. Consider the growth of a spherical tissue  $T$  located at the center of a spherical compartment of finite volume, filled with another tissue  $H$  of lower homeostatic pressure. The spherical tissue can be either a primary tumor developing within the tissue it stems from, or a metastasis that has migrated from its original location and invaded a foreign organ. The two tissues are in mechanical contact, so that the total stress is continuous at the interface. Eqs. (1)-(4) must be solved for both compartments, taking the location of the interface of the two tissues into account. A numerical solution of the associated generic growth dynamics is presented in Fig. 2. The solution shows that the tissue with higher homeo-

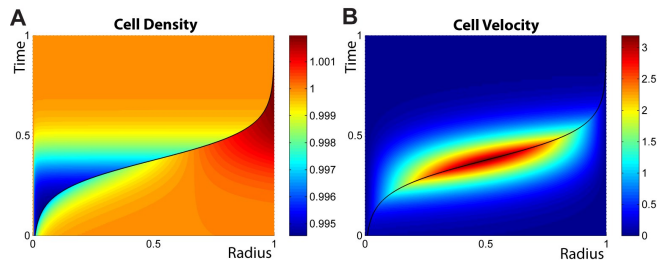


FIG. 2: Numerical solution for the cell density (A) and cell velocity (B) as functions of space and time during the growth of one tissue located in the bulk of another tissue of lower homeostatic pressure. Color coding for local cell density and velocity is given on the right hand side of panels (A) and (B), respectively. Spherical symmetry is assumed. Total integration time, compartment size and homeostatic densities of tissues  $T$  and  $H$  are scaled to one. In both plots, the boundary between the two tissues is indicated by a black line. Parameters are chosen in order to illustrate the interplay between viscous dynamics and compartment growth (see supplementary material).

static pressure grows at the expense of the other one and takes over the entire compartment. *In vivo* however, the condition of a fixed finite volume does not hold in general. In real tissues, there is often first a displacement of the non tumor tissue before anatomical constraints limit the total volume available to the system. However, the devastating effect of malignant tumors stems from the fact that they invade and replace the functional tissues. The architecture of most tissues leads to a competition for volume in the case of neoplastic proliferation. Note that, considering the time evolution of the boundary between the two tissues only, we get a curve that is reminiscent of the well-known, experimentally-observed Gompertzian growth curves (Molski and Konarski, 2003). A quantitative illustration of this behavior obtained within our framework is illustrated in the supplementary material, making use of realistic parameters.

We now examine several effects that can significantly

alter the tumor growth dynamics as presented above. A first example, which is motivated by the structure of benign tumors, corresponds to tissue  $T$  engulfed in a membrane, typically a thin shell of extracellular matrix, where the surface tension  $\gamma$  rises as  $T$  expands. If this tension increases faster than the radius of  $T$ , the additional pressure increases and the expansion of  $T$  eventually stops: a stable steady state exists at  $r = r_s$  such that  $p_{T,h} - p_{H,h} = 2\gamma(r_s)/r_s$ , where  $p_{T,h}$  and  $p_{H,h}$  are the respective homeostatic pressures of  $T$  and  $H$ . A numerical solution illustrating this case is presented in Fig. 3. This

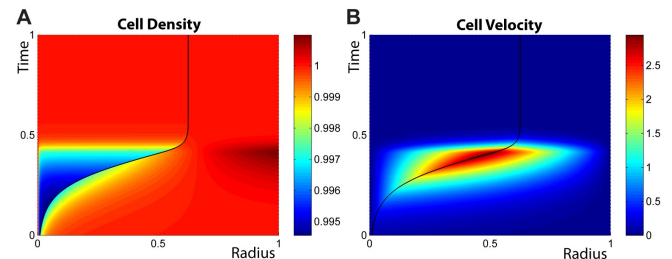


FIG. 3: Numerical solution for the cell density (A) and cell velocity (B) as functions of space and time during the growth of a tissue engulfed in an elastic membrane, and located in the bulk of another tissue of lower homeostatic pressure. As in Fig. 2, spherical symmetry is assumed; total integration time, compartment size and homeostatic densities are scaled to one, and in both plots the boundary between the two tissues is indicated by a black line. Color coding is similar to the one used in Fig. 2. In this solution, the membrane is treated as purely elastic and is put under tension above a given radius  $x_0 = 0.5$ . The explicit surface tension dependence on the boundary location  $x$  is given in the supplementary material. Additional parameters are given in the supplementary material. (A) The expansion of the inner compartment is similar to that of Fig. 2 until, at  $x = 0.5$ , surface tension begins to play a role. The membrane expands until its tension balances the pressure difference between the two compartments and a stable steady state is reached. (B) Corresponding cell-velocity plot.

dormant state is stable until genetic alterations inducing the production of proteases by the tumor cells lead to the degradation of the membrane.

As a second example, we consider the case of a tumor that is limited in its growth, for example by nutrient or oxygen supply. It is indeed a well-known fact that tumors are poorly vascularized before they acquire the capability to trigger the growth of new blood vessels via angiogenesis (Folkman and D'Amore, 1996; Weidner, 1991; Hanahan and Weinberg, 2000). This limitation has profound consequences for their growth dynamics (Preziosi, 2003), often leading to the existence of a maximum size of about one to two millimeters, where they remain in a “dormant state” until the induction of angiogenesis (Folkman and D'Amore, 1996; Weinberg, 2007). In Fig. 4, we present a numerical integration of the growth dynamics of a nutrient-limited tumor in the bulk of a healthy, well vascularized tissue. While we assume a homoge-

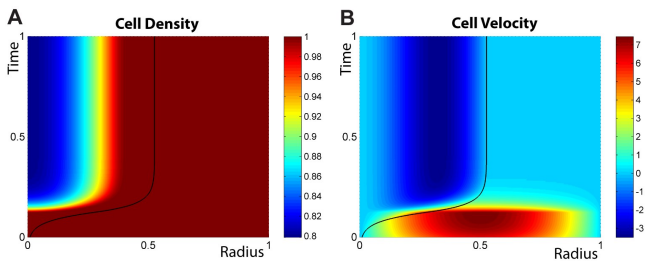


FIG. 4: Numerical solution of the growth dynamics with the geometrical arrangement of Fig. 2 when growth rates are nutrient-limited. Nutrients diffuse into the inner compartment through the tissue interface (see supplementary material). (A) The inner compartment starts growing as in the case of Fig. 2 but asymptotically reaches a maximum size. (B) Cells proliferate at the surface of the inner compartment which is rich in nutrients and die at the center where nutrients are scarce, resulting in an inward flow of cells. Color coding is similar to the one used in Fig. 2 and 3, but it now allows for negative values required by the inward flow.

neous and high enough concentration of nutrients for the healthy tissue, the neoplastic tissue is only supplied with nutrients via diffusion through its surface. Since nutrient diffusion is fast compared to growth dynamics, we calculate the nutrient concentration profile by solving a steady-state diffusion equation, taking into account nutrient consumption due to cell metabolism and division (see supplementary material). We choose functional dependences of the division and apoptosis rates on the nutrient concentration and cell density that correspond to a biological behavior: under very low concentrations of nutrients or oxygen, cells tend to die, but a limited supply of nutrients can also decrease cell division by triggering cell differentiation, inducing a quiescent cell state or favoring adaptation of the metabolism of the cells to the new environment. In agreement with what is known about the internal structure of dormant tumors, cells divide at the boundary where they get enough nutrients, and die at the center. This creates a steady state flow of cells from the surface toward the center of the tumor and thereby a constant cell turnover that is favorable to mutations.

Note that the typical length-scale at which the diffusion of nutrients becomes a limiting factor is of the order of millimeters, the size of a dormant tumor (Folkman and D’Amore, 1996; Weinberg, 2007). This scale is very large compared to the size we estimate for the critical radius introduced above. In the following, when considering the nucleation process of micro-tumors, we therefore assume a homogeneous, high enough concentration of nutrients.

### Critical Size and Stochastic Growth Dynamics

A third effect that can modify tumor growth dynamics is the presence of a constant tissue interfacial tension as introduced above. When  $H$  and  $T$  are at their homeostatic densities, there exists a particular radius  $r_c$  at

which mechanical equilibrium is reached, but this equilibrium, given by  $p_{T,h} - p_{H,h} = 2\gamma/r_c$ , is unstable. Numerical solutions illustrating the growth dynamics around this critical radius are presented in Fig. 5.

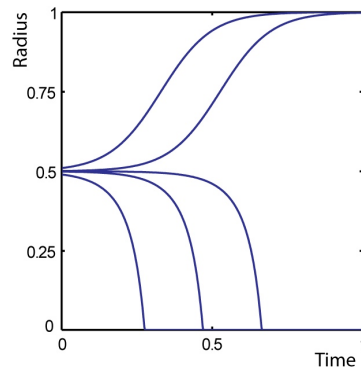


FIG. 5: Tissue boundary as a function of time during the growth of a tissue located in the bulk of another tissue of lower homeostatic pressure, with interfacial tension and in spherical geometry. Parameters are given in the supplementary material, together with  $r_c = 0.5$  and  $\gamma = 1$ . The different curves show the dynamics for the following initial values  $r_0$  of  $r$ : 0.49, 0.499, 0.4999, 0.501 and 0.51. Both tissues start out at their homeostatic densities.

Given the existence of such an unstable critical radius, the question arises as to how a metastasis—or a primary tumor—can grow within a healthy tissue since in general it originates from a single cell (Talmadge and Fidler, 1982; Talmadge and Zbar, 1987; Chambers and Wilson, 1988). The answer stems from stochasticity, an aspect of the dynamics that has been ignored in the description so far. The importance of stochasticity in growth processes has already been recognized in various situations (Nowak *et al.*, 2003). Under the assumption that stochastic tumor growth is a Poisson process, the evolution of the probability  $P(n, t)$  for a spherical tumor  $T$  inside a healthy tissue  $H$  to contain  $n$  cells at time  $t$  can be described by a master equation:

$$\frac{dP(n, t)}{dt} = r_{n-1}^+ P(n-1, t) - (r_n^+ + r_n^-) P(n, t) + r_{n+1}^- P(n+1, t), \quad (5)$$

where  $r_n^+ = nk_d$  and  $r_n^- = nk_a$  are the rates at which a tumor grows or shrinks from  $n$  to  $(n+1)$  or  $(n-1)$  cells, respectively. The rates  $k_d$  and  $k_a$  depend on  $n$ , and we model their dependence in the following way: For tumors small compared to the size of the healthy compartment, the healthy tissue is only slightly perturbed away from its homeostatic state. Thus, the pressure inside the tumor is given by Laplace’s law:  $p_T = p_{H,h} + 2\gamma/r$ . Therefore, the division and apoptosis rates of a spherical tumor of radius  $r$  are given by:

$$k_{d/a} = -\kappa_{d/a} \chi_T \left( p_{H,h} + \frac{2\gamma}{r} - p_{T,h} \right) + k_0. \quad (6)$$

Here,  $\kappa_d$ ,  $\kappa_a$  and  $k_0$  are three phenomenological coefficients that enter the linear expansions of  $k_d$  and  $k_a$ , similarly to  $\kappa$  in Eq. (4). To ensure the proper behavior as a function of the cell density  $\rho$ ,  $\kappa_d$  needs to be positive and  $\kappa_a$  negative. Both equations for  $k_d$  and  $k_a$  share the same constant  $k_0$  such that Eq. (4) is satisfied with  $\kappa = \kappa_d - \kappa_a$ . In the master equation (5), the rates  $r_n^+$  and  $r_n^-$  are then given to leading order by:

$$r_n^{\pm} = n \left[ -\kappa_{d/a} \chi_T \left( p_{H,h} + 2\gamma \left( \frac{4\pi\rho_{T,h}}{3n} \right)^{1/3} - p_{T,h} \right) + k_0 \right], \quad (7)$$

and  $k_0 > 0$  fixes the amount of cell turnover—and thereby the amount of stochasticity—in the system.

For an analytic treatment, we map this growth process onto a random walk with sinks at  $n = 0$  and  $n = n_{\max}$ , which results in a linear birth-death process where all tumors either disappear or reach macroscopic sizes when time goes to infinity. The so-called “splitting probability”  $\Pi_g$ —namely the probability for a single cell to reach the size  $n = n_{\max}$  and not disappear in the lower sink  $n = 0$ —is given by (Van Kampen, 2007):

$$\Pi_g = \frac{1}{1 + \sum_{\mu=1}^{n_{\max}-1} \frac{r_{\mu}^- r_{\mu-1}^- \dots r_1^-}{r_{\mu}^+ r_{\mu-1}^+ \dots r_1^+}}. \quad (8)$$

In Fig. 6, we present this analytic result together with the results of a Monte Carlo simulation of Eqs. (5)-(7) based on a Gillespie algorithm (Gillespie, 1977).

Finally, it is interesting to consider the growth of neoplastic semi-spheroids on tissue boundaries. The internal pressure of a semi-spheroid is again given by Laplace’s law, but for the same radius, the number of cells within the tumor is half that of a complete spheroid. Therefore, the critical number of cells of a tumor at an interface is only half that of a tumor in the bulk. We can directly read the resulting effect on the growth probability out of Fig. 6. For example, between the critical sizes of five and ten cells, we obtain a growth probability ratio of 8.6. This characterizes a significant preference for tumors to grow on surfaces, an effect that has been observed experimentally (Cameron *et al.*, 2000) and clinically (Weiss, 1985). Note that other mechanisms—such as the adhesion of cancerous cells to the extracellular matrix, which leads to a different initial distribution of metastatic cells—might also play a role.

## Discussion

In this work, we have shown that homeostatic regulation of cell density and pressure leads to a competition for space between tissues in mechanical contact. We have proposed that an increased homeostatic pressure is a characteristic trait of tumors. Gedanken experiments

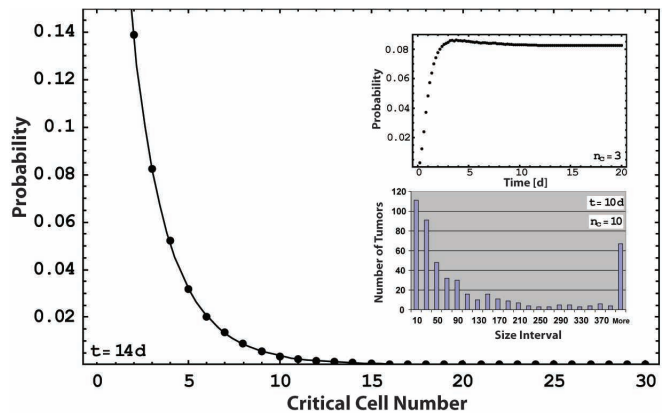


FIG. 6: Splitting probability as a function of the critical cell number. The black dots are the fraction of tumors with a size larger than the critical radius after 14 days of evolution, starting from a single cell in a Monte Carlo simulation (see Eqs. (5) and (7)). The black line represents the analytic result for the splitting probability as given by Eq. (8). Parameters are chosen such that far above the critical radius the division rate reaches a value of one division per day and the apoptosis rate is negligible.  $k_0$  in Eq. (7) is chosen to be 0.9 division per day. Note that the probability for growth on the compartment surface can be read out from the plot using half of the critical cell number of the process in the bulk. Upper inset: Fraction of tumors that are above the critical size. This fraction relaxes to a constant value in a Monte Carlo simulation. Lower inset: Distribution of tumor sizes in a Monte Carlo simulation after 10 days of evolution of  $10^5$  individual tumor cells.

for measuring the homeostatic pressure and growth rates have been discussed and could be realized using current experimental techniques. For example, Helminger *et al.* have shown that tumors growing in agarose gels proliferate until the pressure exerted by the gel reaches 45-120 mmHg (Helminger *et al.*, 1997). This gives an estimate of the homeostatic pressure defined in this paper. Such numbers are compatible with the pressure typically generated by actin polymerization (Footer *et al.*, 2007; Marcy *et al.*, 2004). An experiment of particular interest that has not been performed so far is the competition between a healthy and a tumor-like tissue separated by a piston, which could prove that mechanical effects are important for tumor growth. If the growth mechanism discussed in this paper is relevant to tumor growth, it would be interesting to measure the homeostatic pressures characterizing healthy and neoplastic tissues, together with their dependences on their biochemical environments. Of particular interest would be their dependence on oxygen, nutrients, growth factors and drugs.

The second concept introduced in this paper is the existence of a critical size for tumor growth due to biochemical, immunological or mechanical surface effects that can outbalance the bulk growth advantage of the neoplastic tissue for small tumor sizes. We show that this interaction can be responsible for the inefficiency of the metastatic cascade after extravasation. The growth of

very few metastases to macroscopic sizes cannot be explained by size-independent growth rates, which yield a probability distribution of metastatic cell clusters that decays exponentially with cluster size. Instead, the existence of a critical size yields realistic values for metastatic inefficiency and a distribution of tumor sizes compatible with experimental observations (Luzzi *et al.*, 1998; Cameron *et al.*, 2000; Zijlstra *et al.*, 2002) (see Fig. 6). Fig. 6 also shows the dependence of metastatic inefficiency on the critical size: a small change in tissue-tumor interaction such as an increased interfacial tension can dramatically lower the probability for macroscopic growth. As an illustration of this effect, consider a metastatic tissue with a critical cell number of 5 in a given environment. Let us compare this situation with that of the same tissue placed in another environment where its interfacial tension is now twice as large, a situation that is well within natural variations (Foty, 1996). While for the first environment, about 3 in 100 metastatic cells form a macroscopic tumor, in the second environment, with a critical cell number of 40, less than 2 in ten million manage to do so. This corresponds to a difference in metastatic efficiency of five orders of magnitude. We propose that this effect could account for the strong tissue specificity of metastatic growth that underlies the “seed and soil hypothesis” (Weinberg, 2007).

The concept of homeostatic pressure presented here is not an alternative to the cellular and genetic mechanisms involved in tumor growth, but rather a different level of description. Indeed, we propose that some of the fundamental biological deregulations that are characteristic of neoplastic cells lead to an increased homeostatic pressure. The framework presented here can be used to explicitly take into account such well-known properties. It can also be generalized to incorporate more general features of biological tissue behavior. For example, on long time scales, genetic instability as well as senescence render tissue properties time dependent. This could be incorporated into our framework using techniques similar to those of Hallatschek *et al.* (Hallatschek *et al.*, 2007; Hallatschek and Nelson, 2008), as well as those of multiscale models of tumor growth (Ribba *et al.*, 2006; Macklin and Lowengrub, 2007; Wise *et al.*, 2008).

### Acknowledgments

We thank M. Bornens, M. Piel and P. Silberzan for many helpful discussions, and P. Janmey for useful comments.

- 
- [1] Cameron, MD, Schmidt, EE, Kerkvliet, N, Nadkarni, KV, Morris, VL, Groom, AC, Chambers, AF, and MacDonald, IC (2000). “Temporal Progression of Metastasis in Lung: Cell Survival, Dormancy, and Location Dependence of Metastatic Inefficiency 1.” *Cancer Research* **60**, 2541–2546.
  - [2] Chambers, AF, Groom, AC, and MacDonald, IC (2002). “Dissemination and growth of cancer cells in metastatic sites.” *Nat Rev Cancer* **2**, 563–572.
  - [3] Chambers, AF, and Wilson, S (1988). “Use of Neo R B16F1 murine melanoma cells to assess clonality of experimental metastases in the immune-deficient chick embryo.” *Clinical and Experimental Metastasis* **6**, 171–182.
  - [4] Chaplain, M. AJ, Graziano, L, and Preziosi, L (2006). “Mathematical modelling of the loss of tissue compression responsiveness and its role in solid tumour development.” *Mathematical Medicine and Biology* **23**, 197–229.
  - [5] Couzin, J (2003). “Tracing the Steps of Metastasis, Cancer’s Menacing Ballet.” *Science* **299**, 1002–1006.
  - [6] Duguay, D, Foty, RA, and Steinberg, MS (2003). “Cadherin-mediated cell adhesion and tissue segregation: qualitative and quantitative determinants.” *Developmental Biology* **253**, 309–323.
  - [7] Engler, AJ, Richert, L, Wong, JY, Picart, C, and Discher, DE (2004). “Surface probe measurements of the elasticity of sectioned tissue, thin gels and polyelectrolyte multilayer films: Correlations between substrate stiffness and cell adhesion.” *Surface Science* **570**, 142–154.
  - [8] Fidler, IJ (2003). “The pathogenesis of cancer metastasis: the seed and soil hypothesis revisited.” *Nat Rev Cancer* **3**, 453–458.
  - [9] Folkman, J, and D’Amore, PA (1996). “Blood vessel formation: what is its molecular basis.” *Blood* **87**, 1153–1155.
  - [10] Footer, MJ, Kerssemakers, J. WJ, Theriot, JA, and Dogterom, M (2007). “Direct measurement of force generation by actin filament polymerization using an optical trap.” *Proc. Natl. Acad. Sci. USA* **104**, 2181–2186.
  - [11] Forgacs, G, Foty, RA, Shafir, Y, and Steinberg, MS (1998). “Viscoelastic Properties of Living Embryonic Tissues: a Quantitative Study.” *Biophysical Journal* **74**, 2227–2234.
  - [12] Foty, RA (1996). “Surface tensions of embryonic tissues predict their mutual envelopment behavior.” *Development* **122**, 1611–1620.
  - [13] Foty, RA, Forgacs, G, Pflieger, CM, and Steinberg, MS (1994). “Liquid properties of embryonic tissues: Measurement of interfacial tensions.” *Physical Review Letters* **72**, 2298–2301.
  - [14] Frisch, U, Hasslache, B, and Pomeau, Y (1986). “Lattice-Gas Automata for the Navier-Stokes Equation.” *Physical Review Letters* **56**, 1505–1508.
  - [15] Gillespie, D. et al. (1977). “Exact stochastic simulation of coupled chemical reactions.” *The Journal of Physical Chemistry* **81**, 2340–2361.
  - [16] Hallatschek, O, Hersen, P, Ramanathan, S, and Nelson, DR (2007). “Genetic drift at expanding frontiers promotes gene segregation.” *Proc. Natl. Acad. Sci. USA* **104**, 19926–19930.
  - [17] Hallatschek, O, and Nelson, DR (2008). “Gene surfing in expanding populations.” *Theoretical Population Biology* **73**, 158–170.
  - [18] Hanahan, D, and Weinberg, RA (2000). “The hallmarks

- of cancer.” *Cell* **100**, 57–70.
- [3] Helmlinger, G, Netti, PA, Lichtenbeld, HC, Melder, RJ, and Jain, RK (1997). “Solid stress inhibits the growth of multicellular tumor spheroids.” *Nature Biotechnology* **15**, 778–783.
- [20] Kong, HJ, Polte, TR, Alsberg, E, and Mooney, DJ (2005). “FRET measurements of cell-traction forces and nano-scale clustering of adhesion ligands varied by substrate stiffness.” *Proceedings of the National Academy of Sciences* **102**, 4300–4305.
- [21] Lecuit, T, and Lenne, PF (2007). “Cell surface mechanics and the control of cell shape, tissue patterns and morphogenesis.” *Nat Rev Mol Cell Biol* **8**, 633–644.
- [22] Luzzi, KJ, MacDonald, IC, Schmidt, EE, Kerkvliet, N, Morris, VL, Chambers, AF, and Groom, AC (1998). “Multistep Nature of Metastatic Inefficiency Dormancy of Solitary Cells after Successful Extravasation and Limited Survival of Early Micrometastases.” *American Journal of Pathology* **153**, 865–873.
- [23] Macklin, P, and Lowengrub, J (2007). “Nonlinear simulation of the effect of the microenvironment on tumor growth.” *Journal of Theoretical Biology* **245** (4), 677–704.
- [24] Marcy, Y, Prost, J, Carlier, MF, and Sykes, C (2004). “Forces generated during actin-based propulsion: A direct measurement by micromanipulation.” *Proc. Natl. Acad. Sci. USA* **101**, 5992–5997.
- [25] Molski, M, and Konarski, J (2003). “Coherent states of Gompertzian growth.” *Physical Review E* **68**, 21916.
- [26] Nowak, M, Michor, F, and Iwasa, Y (2003). “The linear process of somatic evolution.” *Proc. Natl. Acad. Sci. USA* **100**, 14966–14969.
- [27] Preziosi, L, and Press, CRC (2003). “Cancer Modelling and Simulation.” *Cancer Modelling and Simulation*. Chapman & Hall/CRC, Boca Raton, FL.
- [28] Ribba, B, Saut, O, Colin, T, Bresch, D, Grenier, E, and Boissel, JP (2006). “A multiscale mathematical model of avascular tumor growth to investigate the therapeutic benefit of anti-invasive agents.” *Journal of Theoretical Biology* **243**, 532–541.
- [29] Sachs, R, Hlatky, L, and Hahnfeldt, P (2001). “Simple ODE models of tumor growth and anti-angiogenic or radiation treatment.” *Mathematical and Computer Modelling* **33**, 1297–1305.
- [30] Sahai, E (2007). “Illuminating the metastatic process.” *Nat Rev Cancer* **1910**, 737–749.
- [31] Schötz, EM, Burdine, RD, Jülicher, F, Steinberg, MS, Heisenberg, CP, and Foty, RA (2008). “Quantitative differences in tissue surface tension influence zebrafish germ layer positioning.” *HFSP Journal* **2**, 42–56.
- [32] Shraiman, BI (2005). “Mechanical feedback as a possible regulator of tissue growth.” *Proc. Natl. Acad. Sci. USA* **102**, 3318–3323.
- [33] Talmadge, JE, and Fidler, IJ (1982). “Evidence for the clonal origin of spontaneous metastases.” *Science* **217**, 361–363.
- [34] Talmadge, JE, and Zbar, B (1987). “Clonality of pulmonary metastases from the bladder 6 subline of the B 16 melanoma studied by southern hybridization.” *Journal of the National Cancer Institute* **78**, 315–320.
- [35] Van Kampen, NG (2007). “Stochastic Processes in Physics and Chemistry.” North-Holland, Amsterdam.
- [8] Weinberg, RA (2007). “The biology of cancer.” Garland Science, New York, NY.
- [37] Weiss, L (1985). “Principle of Metastasis.” Academic Press, Orlando, FL.
- [38] Wise, SM, Lowengrub, JS, Frieboes, HB, and Cristini, V (2008). “Three-dimensional multispecies nonlinear tumor growth - I. Model and numerical method.” *Journal of Theoretical Biology* **253**, 524–543.
- [39] Zijlstra, A, Mellor, R, Panzarella, G, Aimes, RT, Hooper, JD, Marchenko, ND, and Quigley, JP (2002). “A Quantitative Analysis of Rate-limiting Steps in the Metastatic Cascade Using Human-specific Real-Time Polymerase Chain Reaction 1.” *Cancer Research* **62**, 7083–7092.

# Supplemental Material

## I. SPHERICAL GROWTH

As an example of a tissue growth competition for which we can solve the complete dynamics given by the Eqs. 1-4 of the main text, we examine the growth of a spherical tissue located in the center of a spherical compartment filled with another tissue of lower homeostatic pressure and enclosed by a rigid boundary. For now, we neglect all surface tension effects. The force balance condition (Eq. 2, main text) in three dimensions takes the form:

$$\frac{\partial \sigma'_{rr}}{\partial r} + \frac{2(\sigma'_{rr} - \sigma'_{\theta\theta})}{r} = \frac{\partial p}{\partial r} \quad \sigma'_{\phi\phi} = \sigma'_{\theta\theta}, \quad (9)$$

where  $r$ ,  $\theta$  and  $\phi$  are the spherical coordinates, while the constitutive equation (Eq. 3, main text) reads:

$$\begin{aligned} \sigma'_{rr} &= 2\eta \frac{\partial v}{\partial r} \\ \sigma'_{\theta\theta} &= 2\eta \frac{v}{r}. \end{aligned} \quad (10)$$

The continuity equation (Eq. 1, main text), together with the expansion of  $k_d - k_a$  to first order in  $\rho - \rho_h$  (Eq. 4, main text), gives:

$$\frac{\partial \rho}{\partial t} + \frac{1}{r^2} \frac{\partial}{\partial r} (r^2 \rho v) = -\kappa(\rho - \rho_h)\rho. \quad (11)$$

These equations need to be solved for the whole system composed of the two tissues, together with the moving boundary between them. Boundary conditions are composed of two parts: (a) in the center and at the rigid external wall, the velocity field vanishes, such that  $v(r=0) = v(r=R) = 0$ ; (b) at the interface of the two tissues, the velocity field and the stress tensor are continuous. The continuity of the velocity field at the interface leads to the following equation for the time-dependent location  $x(t)$  of the tissue boundary:

$$\frac{\partial x}{\partial t} = v(x). \quad (12)$$

The force-balance condition (9) can be integrated using:

$$\frac{\partial \sigma'_{\theta\theta}}{\partial r} = \frac{1}{r}(\sigma'_{rr} - \sigma'_{\theta\theta}) \quad (13)$$

from the constitutive equation (10) to give:

$$2\eta \left( \frac{\partial v}{\partial r} + \frac{2v}{r} \right) = p - p_{\text{ext}}. \quad (14)$$

In the absence of surface tension, the integration constant  $p_{\text{ext}}$  is the external pressure imposed by the rigid

wall to satisfy the boundary condition of vanishing velocity. The growth dynamics consisting of Eqs. (11) and (14) for each of the two compartments—together with the moving boundary condition Eq. (12)—can be solved numerically using a finite-difference method (Press *et al.*, 1992). Results with the parameters of Table I are displayed in Fig. 2 of the main text and show how the inner tissue takes over the whole compartment.

In the main text, a constant interfacial tension is introduced between the two tissues. It is shown that this effect leads to the existence of an unstable critical radius in spherical geometry. The growth dynamics with an unstable critical radius is illustrated in Fig. 5 of the main text. However, biologically relevant situations may involve tissues enclosed in membranes whose tensions increase as the inner tissue grows. This is for example the case for some benign tumors that undergo growth arrest due to the extracellular membrane engulfing them. In that case, the surface tension is now dependent on the location  $x$  of the boundary between the two tissues. For a purely elastic membrane that is put under tension above a given radius  $x_0$ , we have:

$$\gamma(x) = \gamma_0 \frac{(x - x_0)^2}{x_0^2} \theta(x - x_0), \quad (15)$$

where  $\theta(x)$  is the heaviside step function. A numerical solution of the growth dynamics with this type of surface tension is presented in Fig. 3 of the main text (parameters are given in Table I together with  $\gamma_0 = 5$  in scaled units).

## II. TUMOR GROWTH DYNAMICS WITH REALISTIC PARAMETERS

The growth rate of tumor cells is possibly very slow compared to the viscous relaxation time. In such a case, it can be assumed that the cell density in each compartment is constant. In the absence of surface tension, the pressures in the two compartments balance, leading to an equation relating the two densities:

$$\chi_H^{-1}(\rho_H - \rho_{H,h}) + p_{H,h} = \chi_T^{-1}(\rho_T - \rho_{T,h}) + p_{T,h}. \quad (16)$$

The change in density in each compartment has contributions coming from the total cell division and apoptosis taking place in the compartment, as well as from the movement of the boundary  $x(t)$ :

$$\begin{aligned} \dot{\rho}_T &= -\kappa_T (\rho_T - \rho_{T,h}) \rho_T - 3 \frac{\dot{x}}{x} \rho_T \\ \dot{\rho}_H &= -\kappa_H (\rho_H - \rho_{H,h}) \rho_H + 3 \frac{\dot{x}}{x} \frac{x^3}{R^3 - x^3} \rho_H. \end{aligned} \quad (17)$$

This system of differential equations can be solved numerically. Results with the parameters given in Table II are displayed in Fig. 7.

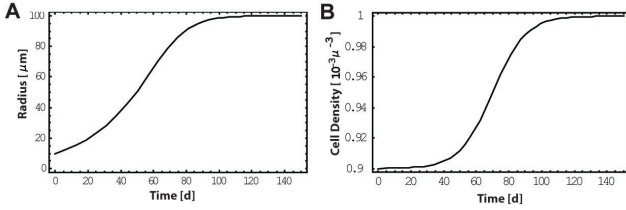


FIG. 7: Radius and cell-density as functions of time for a growing tumor in conditions identical to those of Fig. 2 of the main text, but with estimates of realistic parameters. Cell density is one per  $10^3 \mu\text{m}^3$ , and cell division rate is one per day. The homeostatic pressure difference and the tissue viscosity are  $10^3 \text{ Pa}$  and  $10^4 \text{ Pa}\cdot\text{s}$ , respectively (Helminger *et al.*, 1997; Kruse *et al.*, 2000; Forgacs *et al.*, 1998). Tissue compressibility is  $10^{-7} \text{ Pa}^{-1}\cdot\text{m}^{-3}$  (Tschumperlin *et al.*, 2004). With these parameters, a separation of timescales between the slow cell division and the comparatively fast viscous dynamics occurs, such that we can assume homogeneous cell densities in both compartments. Starting from a single cell and neglecting nutrient coupling, a tumor needs about 100 days to fill a compartment with radius  $100 \mu\text{m}$ .

### III. NUTRIENT-LIMITED GROWTH

When studying the nutrient-limited growth of a tumor prior to angiogenesis, the dependences of the cell division and apoptosis rates  $k_d$  and  $k_a$  on the nutrient and cell densities  $\rho_n$  and  $\rho$  are constructed using two assumptions: (a) below a given concentration of nutrients per cell  $c_1$ , cells stop dividing; (b) below a second, lower concentration of nutrients per cell  $c_2$ , cells undergo apoptosis. We model these properties with the following functions[9]:

$$\begin{aligned}
 k_d &= \frac{\bar{k}_1}{1 + \exp(\alpha(\rho - \rho_h + \Delta\rho))} \times \frac{1}{1 + \exp(-\beta_1(\frac{\rho_n}{\rho} - c_1))} \\
 k_a &= \frac{\bar{k}_1}{1 + \exp(-\alpha(\rho - \rho_h - \Delta\rho))} + \frac{\bar{k}_2}{1 + \exp(\beta_2(\frac{\rho_n}{\rho} - c_2))}.
 \end{aligned}
 \tag{18}$$

Here,  $\bar{k}_1$  tunes the amplitude of cell division and apoptosis in the system as functions of cell density, as  $\bar{k}_2$  tunes how strongly cells die when deprived of nutrients. The parameter  $\alpha$  tunes how sharply cell start to die or proliferate as the homeostatic density is passed. It is the same in both functions  $k_d$  and  $k_a$ , such that  $k_d - k_a = 0$  at  $\rho = \rho_h$  for large concentrations of nutrients.  $\Delta\rho$  sets the amount of cell turnover at homeostatic density. Finally,  $\beta_1$  and  $\beta_2$  tune how sharply the cell division and apoptosis rates change as the critical concentrations of nutrients per cell  $c_1$  and  $c_2$  are passed. We illustrate the dependence of  $k_d$  and  $k_a$  on  $\rho$  and  $\rho_n$  in Fig. 8, with parameters given in Tables I and III. Since only the difference  $k_d - k_a$  enters the growth dynamics (Eq. 1-4, main text),

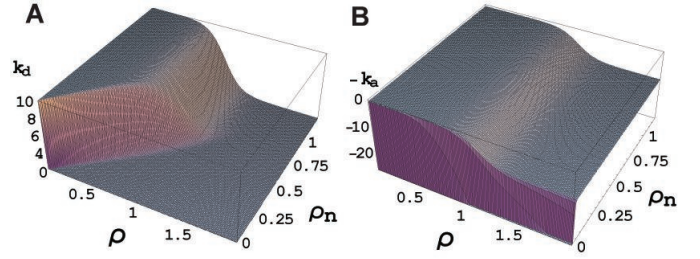


FIG. 8: The cell division rate  $k_d$  (A) and the negative apoptosis rate  $-k_a$  (B) as functions of the cell density  $\rho$  and the nutrient concentration  $\rho_n$ , as given by Eq. (18). Parameters are given in Table III.

we illustrate the dependence of this combination on cell density and nutrient concentration in Figs. 9 and 10.

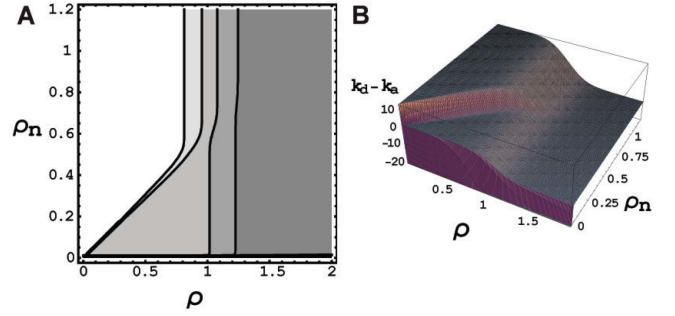


FIG. 9: Difference  $k_d - k_a$  as a function of cell density and nutrient concentration, as given by Eq. (18). Parameters are given in Table III. (A) Top view in grey-scale coding. (B) Three-dimensional view.

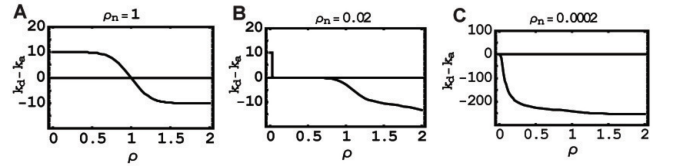


FIG. 10: Effect of nutrient concentration on the difference  $k_d - k_a$  as a function of cell density. Parameters are given in Table III. At high nutrient concentrations, regulation towards the homeostatic density  $\rho_h = 1$  is intact, while at low nutrient concentrations cell division drops significantly. At very low nutrient concentrations, cells undergo apoptosis at a high rate.

To describe how nutrients are distributed in the system, we suppose that they diffuse freely throughout the system with a given diffusion constant  $D_n$ , while being consumed by living cells for their metabolism and their growth. Metabolism uptake happens at a given rate  $\mu\rho_n$  that is proportional to the available concentration of nutrients, and growth dependence is described via an extra consumption term proportional to the number of cell division  $k_d\rho$  with a coupling constant  $\lambda$ . For simplicity, we

suppose no effect of cell apoptosis on nutrient uptake. We finally suppose that nutrient diffusion is very fast compared to tissue growth, such that only the steady-state diffusion equation needs to be considered:

$$D_n \frac{1}{r^2} \frac{\partial}{\partial r} \left( r^2 \frac{\partial \rho_n}{\partial r} \right) - \lambda k_d \rho - \mu \rho_n \rho = 0. \quad (19)$$

Boundary conditions are as follows: the nutrient concentration is homogeneous and constant in the healthy compartment and the flow of nutrients vanishes at the center of the tumor compartment.

To compute the growth dynamics of a spherical tumor coupled to nutrient diffusion through its surface, we use the same method as in Section I, while solving the steady-state diffusion equation (19) at every timestep. The result with the parameters given in Table III is shown in Fig. 4 of the main text. The characteristic nutrient profile in a tumor that is nutrient-limited in its growth is given in Fig. 11.

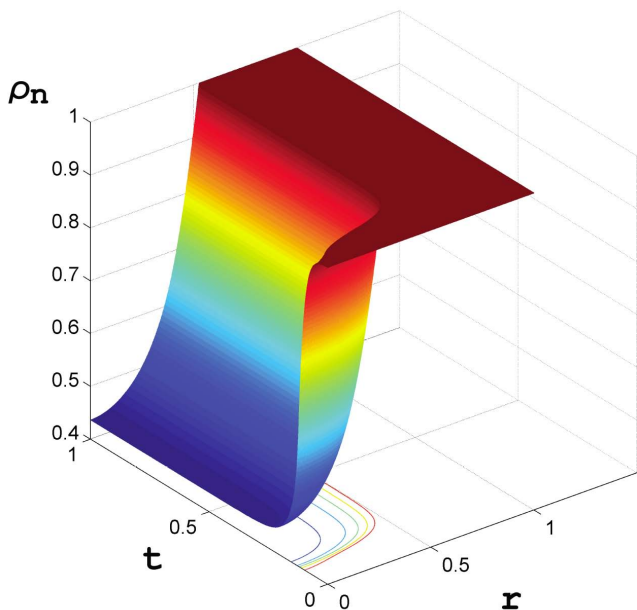


FIG. 11: Typical nutrient profile as a function of time in a growing tumor that arrests in a dormant state. The flux at the center vanishes and the outside compartment has a constant concentration. Parameters correspond to those given in Tables I and III.

#### IV. STOCHASTIC DYNAMICS

We solve the master equation (Eq. 5, main text) together with the rates given by Eq. 7 (main text), both analytically and numerically. Imposing an upper sink at

$n_{\max}$  in addition to the lower sink at  $n_{\min} = 0$ , all clusters of cells end up in one of the two sinks when time goes to infinity. The analytic solution—given by Eq. 8 (main text)—gives the splitting probability, namely the probability for a cluster originating from a single cell to reach the upper sink  $n_{\max}$  when time goes to infinity. Numerically, we use a Monte Carlo simulation of the master equation 5 (main text) based on the Gillespie algorithm (Gillespie, 1976), which gives information on the temporal evolution of the process leading to the analytic result Eq. 8 (main text) for long evolution times.

The Monte Carlo simulation is implemented according to the following standard procedure: at each step of the growth process (corresponding to a new division or apoptosis event), the algorithm first sets the time delay between this event and the previous one, and then chooses whether apoptosis or division takes place. These two choices are made by generating two random numbers  $x_1$  and  $x_2$  in the interval  $[0, 1]$  using a Mersenne Twister algorithm (Matsumoto and Nishimura, 1998).  $x_1$  determines the time delay  $\delta t$  between two events as:

$$\delta t = -\frac{\log(x_1)}{r_n^+ + r_n^-}, \quad (20)$$

where  $r_n^+$  and  $r_n^-$  are the growth and death rates given by Eq. 7 (main text). The stochastic variable  $x_2$  determines whether growth or recession takes place: growth is chosen if  $[(r_n^+ + r_n^-)x_2] \leq r_n^+$ , recession otherwise.

Parameters are chosen as follows: the upper sink is at  $n_{\max} = 10^6$  cells. The parameters that enter the expression for the rates (Eq. 7, main text) are such that, at very large radii, the tumor divides at a rate of one division per day on average, while having a vanishing probability to shrink. This yields:

$$\kappa_{d/a} \chi_T = \frac{k_{n \rightarrow \infty}^{+/-} - k_0}{p_{T,h} - p_{H,h}}, \quad (21)$$

with

$$\begin{aligned} k_{n \rightarrow \infty}^+ &= \lim_{n \rightarrow \infty} \frac{r_n^+}{n} = 1 \\ k_{n \rightarrow \infty}^- &= \lim_{n \rightarrow \infty} \frac{r_n^-}{n} = 0 \end{aligned} \quad (22)$$

in invert units of days. Here,  $k_0$  is an adjustable parameter in the interval  $[k_{n \rightarrow \infty}^-, k_{n \rightarrow \infty}^+]$  that tunes the amount of stochasticity in the system. Finally, we impose a critical radius  $r_c$  corresponding to a critical number of cells  $n_c$  at density  $\rho_{T,h}$ , and choose the surface tension accordingly as:

$$\gamma = \frac{p_{T,h} - p_{H,h}}{2} \left( \frac{3n_c}{4\pi\rho_{T,h}} \right)^{1/3}. \quad (23)$$

The parameters used in Fig. 6 of the main text are given in Table IV.

- 
- [1] Forgacs, G, Foty, RA, Shafir, Y, and Steinberg, MS (1998) Viscoelastic Properties of Living Embryonic Tissues: a Quantitative Study. *Biophysical Journal* **74**, 2227–2234.
- [2] Gillespie, DT (1976) A General Method for Numerically Simulating the Stochastic Time Evolution of Coupled Chemical Reactions. *Journal of Computational Physics* **22**, 403–434.
- [3] Helmlinger, G, Netti, PA, Lichtenbeld, HC, Melder, RJ, and Jain, RK (1997) Solid stress inhibits the growth of multicellular tumor spheroids. *Nature Biotechnology* **15**, 778–783.
- [4] Kruse, SA, Smith, JA, Lawrence, AJ, Dresner, MA, Manduca, A, Greenleaf, JF, and Ehman, RL (2000) Tissue characterization using magnetic resonance elastography: preliminary results. *Phys Med Biol* **45**, 1579–1590.
- [5] Matsumoto, M and Nishimura, T (1998) Mersenne Twister: A 623-Dimensionally Equidistributed Uniform Pseudo-Random Number Generator. *ACM Transactions on Modeling and Computer Simulation* **8**, 3–30.
- [6] Press, WH, Teukolsky, SA, Vetterling, WT, and Flannery, BP (1992) *Numerical recipes in C* Cambridge University Press, Cambridge.
- [7] Tschumperlin, DJ, et al (2004) Mechanotransduction through growth-factor shedding into the extracellular space. *Nature* **429**, 83–86.
- [8] Weinberg, RA (2007). “The biology of cancer.” Garland Science, New York, NY.
- [9] Note that the exact form of these functions is not important. Only their qualitative behavior is relevant.

---

### Tables

Parameter	Value	Description
$x_0$	0.01	initial interface location
$\rho_0$	1	initial density
$v_0$	0	homogeneous initial velocity
$t_{\text{evol.}}$	650	total time of evolution in Fig. 2 (main text)
	600	total time of evolution in Figs. 3 and 5 (main text)
	3000	total time of evolution in Fig. 4 (main text) and Fig. 5 here
$\kappa$	10	division constant (both tissues)
$\chi$	0.2	compressibility (both tissues)
$\eta$	50	viscosity (both tissues)

TABLE I: Parameters used to compute the growth dynamics of spherical tumors in Figs. 2, 3, 4 and 5 of the main text and Fig. 5 here. Parameters are scaled in units of the total compartment size  $R$ , the homeostatic pressure difference  $\Delta p$  between the two tissues and the homeostatic densities  $\rho_h$  which we assume to be identical for the two tissues. Total times are scaled to one in the figures.

Parameter	Value	Description
$R$	100 $\mu\text{m}$	total compartment radius (Weinberg, 2007)
$x_0$	10 $\mu\text{m}$	initial interface location
$\rho_h$	0.001 $\mu\text{m}^3$	homeostatic density (both tissues) (Weinberg, 2007)
$\Delta p$	1000 Pa	difference in homeostatic pressures (both tissues) (Helmlinger <i>et al.</i> , 1997)
$\chi$	$10^{-7} \text{ Pa}^{-1} \cdot \mu\text{m}^{-3}$	compressibility (both tissues) (Tschumperlin <i>et al.</i> , 2004)
$\kappa \cdot \chi \cdot \Delta p$	1 $\text{d}^{-1}$	maximum division rate (both tissues) (Weinberg, 2007)
$\eta$	$10^4 \text{ Pa}\cdot\text{s}$	tissue viscosity (Forgacs <i>et al.</i> , 1998)

TABLE II: List of parameters used to compute the growth dynamics of spherical tumors in Fig. 1.

---

Parameter	Value	Description
$c_1$	0	nutrients per cell for induction of apoptosis
$c_2$	0.6	nutrients per cell for arrest of proliferation
$\bar{k}_1$	10	maximum cell division and apoptosis at high nutrient concentration
$\bar{k}_2$	500	apoptosis rate coefficient at starvation
$\alpha$	10	response coefficient of cell division and apoptosis to cell density
$\beta_1$	50	response coefficient of cell division to nutrient concentration per cell
$\beta_2$	500	response coefficient of cell apoptosis to nutrient concentration per cell
$\Delta\rho$	0.1	shift in cell division and apoptosis tuning the amount of cell turnover at homeostatic density
$D_n$	1	nutrient diffusion constant
$\lambda$	6	nutrient consumption for proliferation
$\mu$	1000	nutrient consumption for metabolism

TABLE III: Parameters used to generate the plots of Fig. 4 of the main text and Figs. 2-5 here in the coupling of the growth dynamics to nutrients as they enter in Eq. (18).

Parameter	Value	Description
$k_{n \rightarrow \infty}^+$	1 d <sup>-1</sup>	$n$ infinity value of $r_n^+/n$
$k_{n \rightarrow \infty}^-$	0 d <sup>-1</sup>	$n$ infinity value of $r_n^-/n$
$k_0$	0.9 d <sup>-1</sup>	cell turnover at homeostatic density

TABLE IV: Parameters used in Fig. 6 of the main text.